

Energy and Age Pareto Optimal Trajectories in UAV-assisted Wireless Data Collection

Yuan Liao and Vasilis Friderikos, *Member, IEEE*

Abstract—This paper studies an unmanned aerial vehicle (UAV)-assisted wireless network, where a UAV is dispatched to gather information from ground sensor nodes (SN) and transfer the collected data to the depot. The information freshness is captured by the age of information (AoI) metric, whilst the energy consumption of the UAV is seen as another performance criterion. Most importantly, the AoI and energy efficiency are inherently competing metrics, since decreasing the AoI requires the UAV returning to the depot more frequently, leading to a higher energy consumption. To this end, we design UAV paths that optimize these two competing metrics and reveal the Pareto frontier. To formulate this problem, a multi-objective mixed integer linear programming (MILP) is proposed with a flow-based constraint set and we apply Bender’s decomposition on the proposed formulation. The overall outcome shows that the proposed method allows deriving non-dominated solutions for decision making for UAV based wireless data collection. Numerical results are provided to corroborate our study by presenting the Pareto front of the two objectives and the effect on the UAV trajectory.

Index Terms—Unmanned aerial vehicle (UAV), Age of information (AoI), energy efficiency, integer programming, Bender’s decomposition.

I. INTRODUCTION

Due to the high flexibility and controllable mobility, one attractive application of unmanned aerial vehicle (UAV) is to serve as a data collector in a wireless sensor network [1]. With the requirement of real-time data transferring and processing, the information freshness is of critical significance for system evaluation, which is hereafter measured by the age of information (AoI) [2]. Besides, due to the limited capacity of the on-board bank of batteries, the aspect of energy efficiency is seen as a key challenge in UAV-enabled wireless networks. Revealing the underlying trade-offs of those two inherently competing metrics is the main focus in this paper. The two extreme points in the Pareto curve is when only the AoI is minimized and when only energy consumption is taken into account. In the first case, the UAV creates a star trajectory meaning that in order to minimize the AoI the UAV returns to the depot every time data are collected from a ground sensor node (SN). On the other extreme, i.e., when energy consumption is only considered the trajectory of the UAV will be a Hamiltonian path that minimize energy consumption. In between those two extreme scenario are the cases where the UAV is return to the depot after serving a subset of SNs. The focus on this work is to reveal the non-dominated operating points in the continuum between those two extreme points of operation.

The authors are with the Department of Engineering, King’s College London, London WC2R 2LS, U.K (e-mail: yuan.liao@kcl.ac.uk; vasilis.friderikos@kcl.ac.uk).

Several existing works concentrated on the information freshness, ie., AoI, in UAV-aided wireless networks. In [3], a UAV is applied to collect data from a group of SNs and then return to a depot for further processing; in this use case scenario the UAV path is designed with the consideration of maximum AoI and average AoI, respectively. The following works extend this model to a multi-UAV use case in [4] and multiple data acquisition mode of operation [5]. In [6], the data collection points, at which the UAV hovers when gathering information, are first obtained through an affinity propagation based algorithm, and then the UAV visits all collection points with the aim of minimizing the AoI. In [7], [8], the UAV is deployed as a relay between a source node and a destination node, and the focus is to provide efficient trajectory design in order to minimize the peak AoI. An AoI-aware drone trajectory is designed through reinforcement learning based approach in [9], [10]. Furthermore, instead of collection data from SNs, the UAV is applied to sense information from target area directly and the trade-off between the sensing and communication is investigated in [11].

In parallel, several existing research works investigated the energy-efficient path planning for UAVs acting as base stations since the on-board battery limitation is one of the key challenges in UAV-assisted networks. In [12], UAVs are deployed to collect information from a group of moving ground devices, in which the energy-aware trajectory is designed through optimal transport theory. The time deadline is considered jointly with the data collection task in [13]. The single UAV case is investigated in [14]. In [15], the hovering points are first solved based on an artificially created energy map and the trajectory is then designed with energy awareness. Furthermore, the closely relevant problem of energy trade-off between the UAV and ground terminals is studied in [16].

Contributions: To minimize the AoI, the UAV is required to offload collected data before sensing/collecting the next one in [11]. Undoubtedly, this type of serving mode has a significantly high energy consumption due to the required flying distance by the UAV. Conversely, the mode proposed in [3] limits the UAV returning to the depot only when all nodes have been visited. This mode of operation certainly improves the energy efficiency at the cost of a higher AoI value. Considering this explicit trade-off between energy consumption and AoI, we propose a multi-return-allowed mode of operation to capture a balance between these two metrics, in which the UAV is allowed to return back to the depot at any time during the serving period. To the best of our knowledge, this is the first work exploiting the trade-off between energy and AoI to reveal the Pareto front and hence allowing to create non-dominated decision making on the trajectory planning.

Furthermore, although the AoI-aware path has been considered in previous works [3]–[6], none of them reveal the Pareto curve that shed light on the trade-offs between energy consumption and AoI and in addition to that these works considered only Hamiltonian paths whereas this work allows returns to depot during a serving cycle. Due to that characteristic these previous works can be considered as a special case of our proposed framework. More specifically, we propose a multi-objective mixed integer linear programming (MILP) formulation based on a flow-based constraint set, in which the flow variables are not only used to eliminate the illegal tours, but also applied to calculate the average AoI. Numerical results show that the multi-return-allowed mode can achieve the Pareto optimal trade-off between the two competing metrics, and illustrate the effects of the UAV speed.

II. SYSTEM MODEL AND PROBLEM FORMULATION

Hereafter, we consider a wireless sensor network with K SNs denoted by the set $\mathcal{K} = \{1, 2, \dots, K\}$, the cartesian coordinates of which are known and fixed at $\mathbf{w}_i \in \mathbb{R}^2$, $\forall i \in \mathcal{K}$. A rotary-wing UAV acts as a flying base station to gather information from all SNs when hovering above them and then transmit/offload the data to the depot that located at $\mathbf{w}_0 \in \mathbb{R}^2$. For notational convenience, we combine the depot and SNs to form an extended set $\mathcal{K}^a = \{0\} \cup \mathcal{K}$, in which the depot is indexed by 0. Unlike the previous works in [3], [5], in which the UAV would not return to the depot until visiting all SNs, our proposed mode allows for a more general case where the UAV is allowed to return back to the depot at any time during the serving cycle, which is hence named as multi-return-allowed serving mode in the rest of the paper.

A. Communication and Energy Consumption Model

In this paper, the fly-hover-communication protocol proposed in [17] is adopted for the communication between UAV and SNs, in which the UAV could gather information only when hovering. Without loss of generality, the UAV is assumed to fly at a fixed altitude H during the flight. Thus, the achievable rate R for the communication between UAV and SNs is assumed to follow the free-space path loss model as,

$$R = B \log_2 \left(1 + \frac{P^t \rho_0}{\sigma^2 H^2} \right), \quad (1)$$

where B is the available bandwidth for communication, P^t is the transmission power of SNs, ρ_0 is the reference channel power gain at $1m$ distance and σ^2 is the power of channel noise. Furthermore, the hovering duration when the UAV collects data from SN i can be calculated by $T_i^h = D_i / R$, where D_i is the data size to be uploaded from SN i . Accordingly, the energy consumption of the UAV when hovering and gathering data from SN i can be calculated by $E_i^h = P^h T_i^h$, where P^h is the hovering power of the UAV.

The UAV is assumed to keep a fixed speed V so that the flying time between two adjacent SNs can be calculated by $T_{ij}^f = \|\mathbf{w}_i - \mathbf{w}_j\| / V$, where $\|\cdot\|$ denotes the 2-norm for a vector. The corresponding energy consumption is $E_{ij}^f = P^f T_{ij}^f$,

where P^f is the propulsion power of the UAV¹. Subsequently, we define a graph $\mathcal{G} = (\mathcal{K}^a, \mathcal{E})$, where \mathcal{E} denotes the set of edges, that is, $\mathcal{E} \triangleq \{(i, j) \mid \forall i, j \in \mathcal{K}^a, i \neq j\}$. For clarity of exposition, the hovering time and energy consumption at the depot is seen as 0, that is, $T_i^h = 0$ and $E_i^h = 0$. Accordingly, we associate the time consumption to the edge (i, j) as,

$$T_{ij} = T_i^h + T_{ij}^f \\ = \begin{cases} \frac{\|\mathbf{w}_i - \mathbf{w}_j\|}{V} & \text{if } i = 0, (i, j) \in \mathcal{E} \\ \frac{D_i}{B \log_2 \left(1 + \frac{P^t \rho_0}{\sigma^2 H^2} \right)} + \frac{\|\mathbf{w}_i - \mathbf{w}_j\|}{V} & \text{if } i \neq 0, (i, j) \in \mathcal{E} \end{cases} \quad (2)$$

Similarly, the energy consumption for edge (i, j) is defined as,

$$E_{ij} = E_i^h + E_{ij}^f \\ = \begin{cases} \frac{P^f \|\mathbf{w}_i - \mathbf{w}_j\|}{V} & \text{if } i = 0, (i, j) \in \mathcal{E} \\ \frac{P^h D_i}{B \log_2 \left(1 + \frac{P^t \rho_0}{\sigma^2 H^2} \right)} + \frac{P^f \|\mathbf{w}_i - \mathbf{w}_j\|}{V} & \text{if } i \neq 0, (i, j) \in \mathcal{E} \end{cases} \quad (3)$$

Note that both T_{ij} and E_{ij} can be seen as constants once the environment is given. The energy consumption for a given trajectory \mathcal{Q} can be calculated as $E = \sum_{(i,j) \in \mathcal{Q}} E_{ij}$, where $(i, j) \in \mathcal{Q}$ means that the UAV travels from i to j adjacently; observe that E is a function of \mathcal{Q} .

B. Age of Information (AoI)

We adopt the concept of AoI to measure the freshness of information for each SN, and derive the average AoI among all SNs to evaluate the performance of the system. In a similar manner as in [3]–[6], we ignore the sampling time sampling and establishing communication links, we assume that SN would generate and upload the information immediately when the UAV arrives. Thus, the AoI of SN i is defined as the time interval from when the UAV starts collecting information from i to when it returns to the depot. To describe the AoI mathematically, we first define a sub-tour as a Hamiltonian cycle with the depot as the start (end) vertex. Note that there might be several sub-tours in the solution since the proposed multi-return-allowed mode allows the UAV back to the depot several times. Given a certain sub-tour consisting of r SNs, the UAV visits $i_0 \rightarrow i_1 \rightarrow i_2 \dots \rightarrow i_r \rightarrow i_{r+1}$ in tandem, where $i_0 = i_{r+1} = 0$ and $i_k \in \mathcal{K}, k = 1, 2, \dots, r$. We define the AoI of SNs visited by this sub-tour recursively, that is,

$$\begin{cases} A_{i_r} = T_{i_r 0} \\ A_{i_k} = T_{i_k i_{k+1}} + A_{i_{k+1}}, k = 1, 2, \dots, r-1 \end{cases} \quad (4)$$

Furthermore, the average AoI among all SNs is adopted to evaluate the performance of system, that is,

$$\bar{A} = \frac{1}{K} \sum_{i \in \mathcal{K}} A_i \quad (5)$$

It can be seen that \bar{A} is a function of the UAV trajectory. However, since there is not an explicit expression of the trajectory,

¹The propulsion power P^f of a rotary-wing UAV is a function of its speed [17], [18]. However, in this paper, the speed is seen as fixed so and the discussion of different speed is illustrated in Section IV.

(5) is challenging to be formulated. However, Theorem 4 in [3] provides an alternative expression of \bar{A} when the trajectory \mathcal{Q} is given, that is,

$$\bar{A} = \sum_{(i,j) \in \mathcal{Q}} \frac{f_{ij}}{K} T_{ij} \quad (6)$$

where f_{ij} denotes the number of visited SNs during the period between the most recent departing from the depot and arriving at j . For instance, given a sub-tour as $i_0 \rightarrow i_1 \rightarrow i_2 \dots \rightarrow i_r \rightarrow i_{r+1}$ where $i_0 = i_{r+1} = 0$, we have $f_{i_0 i_1} = 0$, $f_{i_1 i_2} = 1, \dots, f_{i_r i_{r+1}} = r$.

C. Flow-based Constraint Set and Problem Formulation

In the proposed multi-return-allowed mode, frequent returns of the UAV to the depot result in smaller average AoI, at the cost of an increased energy consumption due to the longer flying distance. As mentioned, both the average AoI and energy consumption are the function of UAV trajectory, and the trade-off between them is mainly discussed in this letter. With this in mind, a multi-objective optimization problem is formulated based on a flow-based constraint set, which is proposed to model the nominal Travelling Salesman Problem (TSP) initially in [19].

$$(P1) : \min_{\mathbf{X}} \sum_{(i,j) \in \mathcal{E}} E_{ij} x_{ij} \quad (7a)$$

$$\min_{\mathbf{Y}} \sum_{(i,j) \in \mathcal{E}} T_{ij} \frac{y_{ij}}{K} \quad (7b)$$

$$s.t. \quad \sum_{i \in \mathcal{K}} x_{0i} = \sum_{i \in \mathcal{K}} x_{i0} \quad (7c)$$

$$\sum_{i \in \mathcal{K}^a} x_{ij} = 1, \forall j \in \mathcal{K} \quad (7d)$$

$$\sum_{i \in \mathcal{K}^a} x_{ji} = 1, \forall j \in \mathcal{K} \quad (7e)$$

$$\sum_{(i,j) \in \mathcal{E}} y_{ij} - \sum_{(j,i) \in \mathcal{E}} y_{ji} = 1, \forall i \in \mathcal{K} \quad (7f)$$

$$y_{oi} = 0, \forall i \in \mathcal{K} \quad (7g)$$

$$0 \leq y_{ij} \leq K x_{ij}, \forall (i,j) \in \mathcal{E} \quad (7h)$$

$$x_{ij} \in \{0, 1\}, \forall (i,j) \in \mathcal{E} \quad (7i)$$

where x_{ij} are binary variables and $x_{ij} = 1$ represents that the edge (i,j) is travelled by the UAV, y_{ij} are the flow variables associated to all edges, $\mathbf{X} \triangleq \{x_{ij} \mid (i,j) \in \mathcal{E}\}$ and $\mathbf{Y} \triangleq \{y_{ij} \mid (i,j) \in \mathcal{E}\}$ are the set of variables. Observe that (7c)-(7e) impose the degree constraints for all SNs and depot. Also, (7i) reflects the binary restriction for the variable x_{ij} . The following two Lemmas illustrate how the constraints (7f)-(7h) operate for the aforementioned multi-return-allowed mode.

Lemma 1: *The constraint (7f) guarantees that if a vertex set $\mathcal{K}' \subseteq \mathcal{K}^a$ constitutes a cycle, the depot must be included by \mathcal{K}' , i.e. $0 \in \mathcal{K}'$.*

Proof: We prove this by induction. Assume that there is a cycle without the depot, we simply choose a SN $i_1 \in \mathcal{K}'$ as the start and end point. Thus, all SNs in this \mathcal{K}' are visited in tandem and let us denote the path as $i_1 \rightarrow i_2 \rightarrow \dots \rightarrow i_r \rightarrow i_1$.

Now let us define $y_{i_1 i_2} = c$. According to the (7f), it follows that, $y_{i_2 i_3} = c + 1, \dots, y_{i_r i_1} = c + r - 1$. Therefore, we have

$$\sum_{(i_1,j) \in \mathcal{E}} y_{i_1 j} - \sum_{(j,i_1) \in \mathcal{E}} y_{j i_1} = c - (c + r - 1) \\ = 1 - r \quad (8)$$

which contradicts with (7f). This completes the proof of Lemma 1. \square

Lemma 2: *The constraints (7f)-(7h) guarantee that the following equation is achieved,*

$$y_{ij} = \begin{cases} f_{ij}, & \text{if } x_{ij} = 1 \\ 0, & \text{otherwise} \end{cases} \quad (9)$$

Proof: The Lemma 1 shows that a cycle must consist of the depot, which is certainly a sub-tour according to the definition of the sub-tour in section II-B. We choose the depot as the start (end) point, thus, the UAV would fly along the trajectory $0 \rightarrow i_1 \rightarrow i_2 \dots \rightarrow i_r \rightarrow 0$. The constraints in (7h) guarantee that y_{ij} can achieve a nonzero value only when $x_{ij} = 1$, otherwise, y_{ij} is forced to 0 when $x_{ij} = 0$. Recalling the constraints (7f) and (7g), we then have $y_{0i_1} = 0, y_{i_1 i_2} = 1, \dots, y_{i_r 0} = r$. Since the inequality $r \leq K$ is held apparently, the constraints (7h) would not be broken when $x_{ij} = 1$. This completes the proof of Lemma 2. \square

Proposition 1: *Problem (P1) solves the proposed multi-return-allowed serving mode with the average AoI and energy consumption as the objective function.*

Proof: According to Lemma 1 and constraints (7c)-(7e), the UAV would visit each SN exactly once and be allowed to return to the depot several times. Lemma 1 also shows the fact that the cycles without the depot are eliminated by (7f). Besides, the first objective function (7a) calculates the energy consumption E . Referring to the equation (6) and Lemma 2, the second objective function (7b) calculates the average AoI \bar{A} . This completes the proof of Proposition 1. \square

Although the path planning problem with AoI and energy consideration is NP-hard, proposing a MILP formulation allows us to solve it efficiently by commercial solvers, such as Gurobi [20]. Also, the proposed flow-based formulation can be easily extended to characterize other AoI-aware path planning problem in aforementioned existing papers. For example, the previous paper [3] limits the UAV back to the depot after all SNs been visited, which mode can be formulated as a MILP by removing the energy objective (7a) and replacing the constraint (7c) by $\sum_{i \in \mathcal{K}} x_{0i} = 1, \sum_{i \in \mathcal{K}} x_{i0} = 1$.

III. SINGLE OBJECTIVE AND BENDER'S DECOMPOSITION

Hereafter we transform (P1) to a single objective problem via the weighted linear combination technique and apply Bender's decomposition to decentralize the overall computational burden when the problem scale is large.

A. Weighted Linear Combination

To combine the objective functions (7a) and (7b), we simply associate each of them with a weighting coefficient and minimize the weighted sum, that is,

$$(P2) : \min_{\mathbf{X}, \mathbf{Y}} \lambda \frac{\sum_{(i,j) \in \mathcal{E}} T_{ij} \frac{y_{ij}}{K} - \bar{A}_{\min}}{\bar{A}_{\max} - \bar{A}_{\min}}$$

$$+ (1 - \lambda) \frac{\sum_{(i,j) \in \mathcal{E}} E_{ij} x_{ij} - E_{min}}{E_{max} - E_{min}} \quad (10a)$$

$$s.t. \quad (7c) - (7i) \quad (10b)$$

where \bar{A}_{min} and \bar{A}_{max} are the minimal and maximal achieved value of \bar{A} respectively, E_{min} and E_{max} are the minimal and maximal energy consumption respectively, λ and $(1 - \lambda)$ denote the weights of two matrices. The Theorem 4 in [21] shows that the solution of (P2) is Pareto optimal if $\lambda \in [0, 1]$.

To derive an explicit expression of the objective function in (P2), the extreme values of \bar{A} and E should be obtained firstly. Since $\{T_{ij} \mid \forall (i, j) \in \mathcal{E}\}$ satisfy the triangle inequality, the UAV would return to the depot immediately after visiting each SN to minimize \bar{A} . In other words, \bar{A}_{min} can be calculated by,

$$\bar{A}_{min} = \sum_{i \in \mathcal{K}} T_{i0} \quad (11)$$

It is observed that the corresponding energy consumption is certainly the maximal value of E , that is,

$$E_{max} = \sum_{i \in \mathcal{K}} (E_{0i} + E_{i0}) \quad (12)$$

Similarly, as shown in (3), $\{E_{ij} \mid \forall (i, j) \in \mathcal{E}\}$ satisfy the triangle inequality and are monotonically increasing of $\|\mathbf{w}_i - \mathbf{w}_j\|$. Therefore, the most energy-efficient path would include exactly one cycle with the shortest flying distance, that is, a TSP solution. The corresponding average AoI can be seen as \bar{A}_{max} . Notably, although TSP is a NP-hard problem, it has been well researched so that we assume that the TSP solution, as well as its corresponding E_{min} and \bar{A}_{max} , are known hereafter.

B. Applying Bender's Decomposition

For notational convenience, we ignore the constant terms in (10a) and rewrite (P2) as,

$$(P3) : \min_{\mathbf{X}, \mathbf{Y}} \sum_{(i,j) \in \mathcal{E}} C_{ij}^T y_{ij} + \sum_{(i,j) \in \mathcal{E}} C_{ij}^E x_{ij} \quad (13a)$$

$$s.t. \quad (7c) - (7i) \quad (13b)$$

where $C_{ij}^T \triangleq \lambda T_{ij} / (K \bar{A}_{max} - K \bar{A}_{min})$ and $C_{ij}^E \triangleq (1 - \lambda) E_{ij} / (E_{max} - E_{min})$ are coefficients defined for simplicity.

Bender's decomposition is a promising approach for large-scale MILP [22], and it has been successfully employed in solving a wide array of optimization design problems in communication networks [23]. To apply Bender's decomposition, we first rewrite (P3) as the following (P4) without loss of optimality,

$$(P4) : \min_{\mathbf{X}} \sum_{(i,j) \in \mathcal{E}} C_{ij}^E x_{ij} + g(\mathbf{X}) \quad (14a)$$

$$s.t. \quad (7c) - (7e), (7i) \quad (14b)$$

where $g(\mathbf{X})$ is defined to be the optimal solution of the following problem,

$$(P5) : \min_{\mathbf{Y}} \sum_{(i,j) \in \mathcal{E}} C_{ij}^T y_{ij} \quad (15a)$$

$$s.t. \quad (7f) - (7h) \quad (15b)$$

(P5) is certainly a linear programming with respect to \mathbf{Y} for given value of $x_{ij} \in \mathbf{X}$. Then, write the dual for (P5) as,

$$(P6) : \max_{\{\alpha_i\} \cup \{\beta_i\} \cup \{\gamma_{ij}\}} \sum_{i \in \mathcal{K}} \alpha_i - \sum_{(i,j) \in \mathcal{E}} K x_{ij} \gamma_{ij} \quad (16a)$$

$$s.t. \quad -\alpha_i + \beta_i - \gamma_{0i} \leq C_{0i}^T, \forall i \in \mathcal{K} \quad (16b)$$

$$\alpha_i - \gamma_{i0} \leq C_{i0}^T, \forall i \in \mathcal{K} \quad (16c)$$

$$\alpha_i - \alpha_j - \gamma_{ij} \leq C_{ij}^T, \forall (i, j) \in \mathcal{E}, i \neq 0, j \neq 0 \quad (16d)$$

$$\gamma_{ij} \geq 0, \forall (i, j) \in \mathcal{E}, \quad (16e)$$

where $\{\alpha_i \mid i \in \mathcal{K}\}$, $\{\beta_i \mid i \in \mathcal{K}\}$ and $\{\gamma_{ij} \mid (i, j) \in \mathcal{E}\}$ are dual variables. The key observation is that the constraints (16b)-(16e) are not related to the values of \mathbf{X} . Suppose the polyhedron constructed by the constraints (16b)-(16e) has M extreme points and N extreme rays. Recalling the polyhedral theories illustrated in the Section I.4.4 of [24], (P6) has an equivalent form as,

$$(P7) : \min_{\theta} \theta \quad (17a)$$

$$s.t. \quad \sum_{i \in \mathcal{K}} \alpha_i^{p,m} - \sum_{(i,j) \in \mathcal{E}} K x_{ij} \gamma_{ij}^{p,m} \leq \theta, \forall m = 1, \dots, M \quad (17b)$$

$$\sum_{i \in \mathcal{K}} \alpha_i^{r,n} - \sum_{(i,j) \in \mathcal{E}} K x_{ij} \gamma_{ij}^{r,n} \leq 0, \forall n = 1, \dots, N \quad (17c)$$

where $(\alpha_1^{p,m}, \dots, \alpha_K^{p,m}, \beta_1^{p,m}, \dots, \beta_K^{p,m}, \gamma_{01}^{p,m}, \dots, \gamma_{K-1K}^{p,m})$ and $(\alpha_1^{r,n}, \dots, \alpha_K^{r,n}, \beta_1^{r,n}, \dots, \beta_K^{r,n}, \gamma_{01}^{r,n}, \dots, \gamma_{K-1K}^{r,n})$ denote the m^{th} extreme point and n^{th} extreme ray of the polyhedra constructed by (16b)-(16e), respectively. And the constraints in (17b) and (17c) are named as optimality and feasibility cuts, respectively. Since (P5) is a linear programming of which the strong duality is held, (P5), (P6) and (P7) achieve the same optimal solution. Therefore, replacing the component $g(\mathbf{X})$ by (P7), (P4) can be rewritten as,

$$(P8) : \min_{\mathbf{X}, \theta} \sum_{(i,j) \in \mathcal{E}} C_{ij}^E x_{ij} + \theta \quad (18a)$$

$$s.t. \quad (7c) - (7e), (7i) \quad (18b)$$

$$(17b) - (17c) \quad (18c)$$

Note that (P3), (P4) and (P8) are equivalent. (P8) and (P5) are always named as master problem and sub-problem, respectively.

However, since the number of the constraints in (17b) and (17c) is extremely large, generating all of them is not practical. To this end, we denote a problem having a similar form as (P8) but do not consist of all constraints in (18c) as the relaxed master problem (RMP). According to the nominal use of Bender's decomposition, adding the optimality and feasibility cuts according to the solution of dual sub-problem (P5) to the RMP and solving it iteratively can converge to the optimal solution; this is due to the fact that the polyhedron constructed by (16b)-(16e) has finite number of extreme points and extreme rays, i.e. $M < \infty$, $N < \infty$ (Corollary 4.4 in the Section I.4.4 of [24]). The procedure of Bender's decomposition is summarized as Algorithm 1, a realization of

Algorithm 1 Applying Bender's Decomposition to (P3)

```

1: Initialize the RMP without any cuts in (18c).
2: repeat
3:   Solve the RMP. Denote the solution as  $\mathbf{X}^*$  and  $\theta^*$ .
4:   Introduce  $\mathbf{X}^*$  to the dual sub-problem (P6). Solve (P6)
   and denote the optimal objective value as  $g(\mathbf{X}^*)$ .
5:   if  $g(\mathbf{X}^*) < \infty$  then
6:     Acquire an extreme point from the solution of (P6)
     and add an optimality cut (17b) to RMP.
7:   else
8:     Acquire an extreme ray and add an feasibility cut
     (17c) to RMP.
9:   end if
10:  until  $g(\mathbf{X}^*) = \theta^*$ 

```

TABLE I
PARAMETER SETTINGS

Parameter	Value	Parameter	Value
B	5 MHz	σ^2	-110 dBm
H	100 m	ρ_0	-60 dB
P^t	0.1 W	D_i	1 Gbits
K	10 (expect Fig.3)	V	[10, 18, 30] m/s
P^h	165 W [17]	P^f	[126, 162, 356] W [17]

which implemented by the Python API of Gurobi 9.1.2 [20] can be found in github.com/Yuanliaoo/BDforUavPath.

IV. NUMERICAL INVESTIGATIONS

In this section, numerical investigations are presented to evaluate the proposed multi-return-allowed framework. The parameter settings are summarized in Table I. As shown in [17], the propulsion power P^f is a non-convex function of speed V . We mainly compare the metrics under the following three typical choices of speed,

- *Maximum-endurance (ME) speed*: The ME speed is the speed that consumes the least energy, in other words, maximizes the UAV endurance under any given on-board energy. Similar as [17], the ME speed and the corresponding propulsion are set as 10 m/s and 126 W, respectively.
- *Maximum-range (MR) speed*: The MR speed is the optimal UAV speed that maximizes the total traveling distance with any given on-board energy. The MR speed and the corresponding propulsion are set as 18 m/s and 162 W, respectively [17].
- *Maximal (MAX) speed*: The MAX speed is the maximal achievable speed of the UAV, which is set as 30 m/s and the corresponding power is 356 W [17].

Fig.1 depict the Pareto front of \bar{A} and E by solving (P2) with different value of λ . The results in Fig.1 are in accordance with the intuition that \bar{A} and E are competing with each other. It is worth pointing out that although we sample the value of $\lambda \in [0, 1]$ every 0.01 to plot Fig.1, the actual results, shown as the small circles, distribute sparsely and overlap. The reason is that both \bar{A} and E are functions of the UAV trajectory, which is formed by the binary variables \mathbf{X} , hence can not change smoothly. Observe that the MR speed results in the most efficient Pareto curve having the best performance on

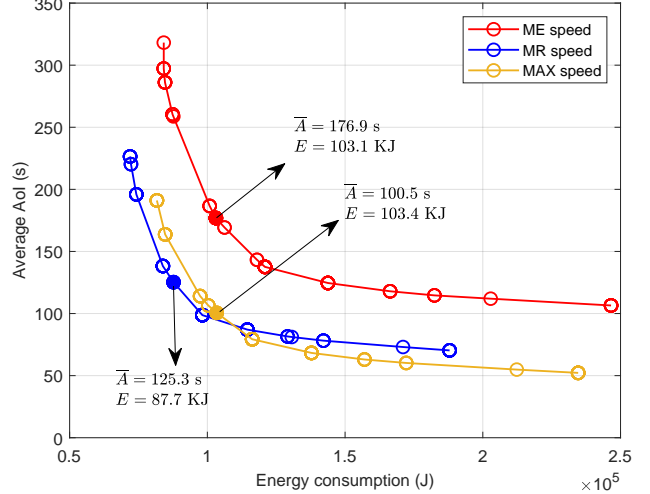


Fig. 1. Pareto front for \bar{A} and E with different speed

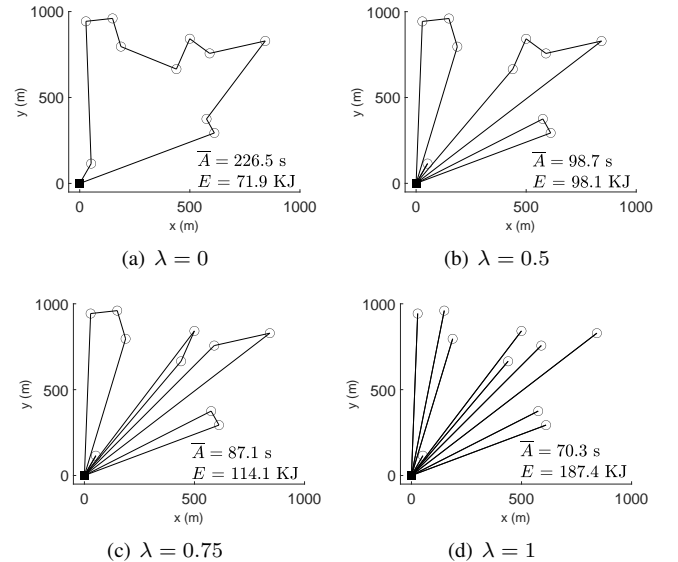


Fig. 2. Comparison of the trajectories as well as \bar{A} and E with different weights λ . Small circles denote SNs and square represents the depot.

both \bar{A} and E ; especially when focusing more to the energy consumption when planning the path, i.e. λ is small. Also, the MAX speed shows competitive performance on both metrics when λ is large. Besides, generating an operating solution from the Pareto front is always meaningful in practice. Thus, we select the solution closest to the utopia point as the operating point under three different speed settings, which are shown as the small solid circles in Fig.1. The performances of those chosen operating points are also shown in Fig.1.

Using the MR speed, the path designs under four different values of λ , 0, 0.5, 0.75 and 1, as well as their corresponding performances are compared in Fig.2. As expected, frequent UAV returns to the depot result in reduced average AoI at the cost of more energy consumption.

In Fig.3 we compare the proposed multi-return-allowed mode (setting $\lambda = 0.5$) with the framework studied in [3], in which the UAV returns to the depot only after all SNs been

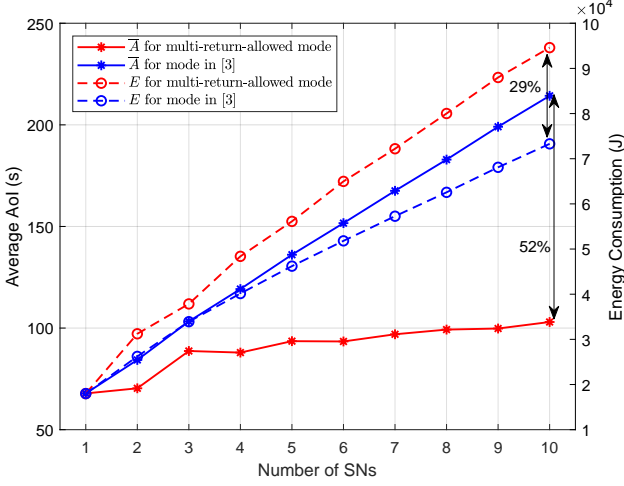


Fig. 3. \bar{A} and E for different serving modes

visited. Note that the energy consumption, shown as the dotted lines in Fig.3, grows almost linearly as the number of SNs increases for both modes. Observing the average AoI, it can be seen that \bar{A} grows linearly when applying the framework in [3], while increases slowly when $K \geq 3$ for the multi-return-allowed mode. In other words, comparing the existing mode, the proposed framework would have a significant gain in \bar{A} when K is large with some additional energy consumption. For example, as shown in Fig.3, there is a 52% gain in \bar{A} with a 29% more energy consumption when $K = 10$.

V. CONCLUSIONS

This paper studies the path planning problem of a UAV-assisted wireless data collection task, in which two inherently competing metrics, namely the average AoI and the aggregate energy consumption, are optimized jointly. To characterize the trade-off between those two performance metrics and reveal the Pareto frontier, we propose a multi-return-allowed serving mode in which the UAV is allowed to return to the depot at any time during the service cycle, and formulate it as a multi-objective MILP with a flow-based constraint set. The two objectives are combined into a single one through the weighted linear combination technique, and apply the Bender's decomposition on the reformulated MILP to decentralize the overall computational burden. By unfolding the Pareto curve the proposed framework allows for deriving non-dominating decision making on the trajectory planning. Additionally, previous research works on Hamiltonian paths only can be considered as a special case of the proposed since it allows multiple returns to the depot during a serving cycle. The numerical results show that the proposed multi-return-allowed mode unveils the trade-off between the two competing metrics and provides non-dominated solutions for advanced decision making.

REFERENCES

- [1] Y. Zeng, R. Zhang, and T. J. Lim, "Wireless communications with unmanned aerial vehicles: Opportunities and challenges," *IEEE Commun. Mag.*, vol. 54, no. 5, pp. 36–42, 2016.
- [2] R. D. Yates, Y. Sun, D. R. Brown, S. K. Kaul, E. Modiano, and S. Ulukus, "Age of information: An introduction and survey," *IEEE J. Sel. Areas Commun.*, vol. 39, no. 5, pp. 1183–1210, 2021.
- [3] J. Liu, X. Wang, B. Bai, and H. Dai, "Age-optimal trajectory planning for UAV-assisted data collection," in *Proc. IEEE Conf. on Computer Commun. Workshops (INFOCOM WKSHPS)*, Honolulu, HI, USA, Apr. 2018, pp. 553–558.
- [4] C. Mao, J. Liu, and L. Xie, "Multi-UAV Aided Data Collection for Age Minimization in Wireless Sensor Networks," in *Proc. Conf. Wireless Commun. Signal Process. (WCSP)*, Changsha, Hunan, China, Oct. 2020, pp. 80–85.
- [5] Z. Jia, X. Qin, Z. Wang, and B. Liu, "Age-based path planning and data acquisition in UAV-assisted IoT networks," in *Proc. IEEE Int. Conf. Commun. Workshops (ICC Workshops)*, Shanghai, China, May 2019, pp. 1–6.
- [6] J. Liu, P. Tong, X. Wang, B. Bai, and H. Dai, "UAV-Aided Data Collection for Information Freshness in Wireless Sensor Networks," *IEEE Trans. Wireless Commun.*, 2020.
- [7] M. A. Abd-Elmagid and H. S. Dhillon, "Average peak age-of-information minimization in UAV-assisted IoT networks," *IEEE Trans. Veh. Technol.*, vol. 68, no. 2, pp. 2003–2008, 2018.
- [8] A. Cao, C. Shen, J. Zong, and T.-H. Chang, "Peak Age-of-Information Minimization of UAV-Aided Relay Transmission," in *Proc. IEEE Int. Conf. Commun. Workshops (ICC Workshops)*, Jun. 2020, pp. 1–6.
- [9] M. A. Abd-Elmagid, A. Ferdowsi, H. S. Dhillon, and W. Saad, "Deep reinforcement learning for minimizing age-of-information in UAV-assisted networks," in *Proc. IEEE Global Commun. Conf. (GLOBECOM)*, Waikoloa, HI, USA, Dec. 2019, pp. 1–6.
- [10] Ferdowsi, Aidin and Abd-Elmagid, Mohamed A and Saad, Walid and Dhillon, Harpreet S, "Neural combinatorial deep reinforcement learning for age-optimal joint trajectory and scheduling design in UAV-assisted networks," *IEEE J. Sel. Areas Commun.*, vol. 39, no. 5, pp. 1250–1265, 2021.
- [11] S. Zhang, H. Zhang, Z. Han, H. V. Poor, and L. Song, "Age of information in a cellular Internet of UAVs: Sensing and communication trade-off design," *IEEE Trans. Wireless Commun.*, vol. 19, no. 10, pp. 6578–6592, 2020.
- [12] M. Mozaffari, W. Saad, M. Bennis, and M. Debbah, "Mobile Internet of Things: Can UAVs provide an energy-efficient mobile architecture?" in *Proc. IEEE Global Commun. Conf. (GLOBECOM)*, Washington, DC, USA, Dec. 2016, pp. 1–6.
- [13] O. Ghdiri, W. Jaafar, S. Alfattani, J. B. Abderrazak, and H. Yanikomeroglu, "Energy-efficient multi-UAV data collection for IoT networks with time deadlines," in *Proc. IEEE Global Commun. Conf. (GLOBECOM)*, Taipei, Taiwan, Dec. 2020, pp. 1–6.
- [14] C. Zhan, Y. Zeng, and R. Zhang, "Energy-efficient data collection in UAV enabled wireless sensor network," *IEEE Wireless Commun. Lett.*, vol. 7, no. 3, pp. 328–331, Jun. 2017.
- [15] L. Shen, N. Wang, Z. Zhu, Y. Fan, X. Ji, and X. Mu, "UAV-enabled Data Collection for mMTC Networks: AEM Modeling and Energy-Efficient Trajectory Design," in *Proc. IEEE Int. Conf. Commun. (ICC)*, Jun. 2020, pp. 1–6.
- [16] D. Yang, Q. Wu, Y. Zeng, and R. Zhang, "Energy tradeoff in ground-to-UAV communication via trajectory design," *IEEE Trans. Veh. Technol.*, vol. 67, no. 7, pp. 6721–6726, Jul. 2018.
- [17] Y. Zeng, J. Xu, and R. Zhang, "Energy minimization for wireless communication with rotary-wing UAV," *IEEE Trans. Wireless Commun.*, vol. 18, no. 4, pp. 2329–2345, Apr. 2019.
- [18] W. Jaafar and H. Yanikomeroglu, "Dynamics of quadrotor UAVs for aerial networks: an energy perspective," *arXiv e-prints*, p. arXiv:1905.06703, May 2019.
- [19] B. Gavish and S. C. Graves, "The travelling salesman problem and related problems," 1978.
- [20] L. Gurobi Optimization, "Gurobi optimizer reference manual," 2021. [Online]. Available: <http://www.gurobi.com>
- [21] A. L. Jaimes, S. Z. Martinez, and C. A. C. Coello, "An introduction to multiobjective optimization techniques," *Optimization in Polymer Processing*, pp. 29–57, 2009.
- [22] J. BnnoBRs, "Partitioning procedures for solving mixed-variables programming problems," *Numerische Mathematik*, vol. 4, no. 1, pp. 238–252, 1962.
- [23] A. Ibrahim, O. A. Dobre, T. M. Ngatchad, and A. G. Armada, "Bender's Decomposition for Optimization Design Problems in Communication Networks," *IEEE Netw.*, vol. 34, no. 3, pp. 232–239, 2019.
- [24] L. A. Wolsey and G. L. Nemhauser, *Integer and combinatorial optimization*. John Wiley & Sons, 1999, vol. 55.